The thymic epithelial microRNA network elevates the threshold for infection-associated thymic involution via miR-29a mediated suppression of the IFN- receptor

Papadopoulou, Aikaterini S ; Dooley, James ; Linterman, Michelle A ; Pierson, Wim ; Ucar, Olga ; Kyewski, Bruno ; Zuklys, Saulius ; Hollander, Georg A ; Matthys, Patrick ; Gray, Daniel H D ; De Strooper, Bart ; Liston, Adrian

Abstract: Thymic output is a dynamic process, with high activity at birth punctuated by transient periods of involution during infection. Interferon- (IFN-) is a critical molecular mediator of pathogen-induced thymic involution, yet despite the importance of thymic involution, relatively little is known about the molecular integrators that establish sensitivity. Here we found that the microRNA network dependent on the endoribonuclease Dicer, and specifically microRNA miR-29a, was critical for diminishing the sensitivity of the thymic epithelium to simulated infection signals, protecting the thymus against inappropriate involution. In the absence of Dicer or the miR-29a cluster in the thymic epithelium, expression of the IFN- receptor by the thymic epithelium was higher, which allowed suboptimal signals to trigger rapid loss of thymic cellularity.

DOI: https://doi.org/10.1038/ni.2193

nature immunology

The thymic epithelial microRNA network elevates the threshold for infection-associated thymic involution via miR-29a mediated suppression of the IFN-α receptor

Aikaterini S Papadopoulou[1,2,9], James Dooley[1,3,9], Michelle A Linterman[4], Wim Pierson[1,3], Olga Ucar[5], Bruno Kyewski[5], Saulius Zuklys[6], Georg A Hollander[6], Patrick Matthys[7], Daniel H D Gray[8], Bart De Strooper[1,2] & Adrian Liston[1,3]

Thymic output is a dynamic process, with high activity at birth punctuated by transient periods of involution during infection. Interferon-α (IFN-α) is a critical molecular mediator of pathogen-induced thymic involution, yet despite the importance of thymic involution, relatively little is known about the molecular integrators that establish sensitivity. Here we found that the microRNA network dependent on the endoribonuclease Dicer, and specifically microRNA miR-29a, was critical for diminishing the sensitivity of the thymic epithelium to simulated infection signals, protecting the thymus against inappropriate involution. In the absence of Dicer or the miR-29a cluster in the thymic epithelium, expression of the IFN-α receptor by the thymic epithelium was higher, which allowed suboptimal signals to trigger rapid loss of thymic cellularity.

Unique among mammalian leukocytes, T cells require a dedicated organ, the thymus, for differentiation. Postnatal thymic output is critical for both effector T cell–mediated immunity[1] and regulatory T cell–mediated tolerance[2]. However, there are circumstances (periodic infection and aging) that drive the process of severe atrophy known as 'thymic involution', which can result in the loss of more than 95% of the cellularity of the thymus. Continued thymic output during such events may be detrimental. The theoretical risk posed by continued thymic function during an infection is that foreign antigens present in the thymus will engender dominant tolerance, protecting the infection from clearance[3]. Thus, thymic involution during infection is a rapid yet transient phenomenon, with recovery within 1–2 weeks[4]. Thymic involution during aging has also been postulated to have biological functions, from acting as a protective mechanism against autoimmunity[5] to allowing optimization of the peripheral repertoire[6] or simply conserving energy by diminishing the inefficient process of T cell differentiation during the decreasing cost-benefit ratio of old age. The kinetics of thymic involution during aging are distinct from those of infection-induced thymic involution, with a gradual progressive decrease in cellularity, at the rate of roughly 1% per year in humans[7].

Characterization of the direct mediators of thymic involution has identified two distinct pathways for this process. The rapid and transient involution initiated during infection can be reproduced by exposure to pathogen-associated molecular patterns (PAMPs) such as poly(I:C)[4]. In this system, thymic involution is dependent on the viral sensor Mda5 and is mediated by the IFNAR1 receptor for interferon-α (IFN-α) expressed on the thymic stroma[4]. Age-related thymic involution, in contrast, is mediated by the sensitivity of thymic epithelial cells to sex hormones[8] and can be reversed by physical or chemical ablation of sex hormones[9]. Other inducers of thymic involution are known, ranging from psychological stress to inflammation[10,11]; however, these phenomena may instead reflect a maladaptive response to noninfectious conditions that mimic signals of infection at the molecular level.

Although the main molecular mediators of infection-induced thymic involution have been identified, the mechanism by which appropriate sensitivity is maintained remains unknown. The thymus has conflicting pressures to ensure rapid involution during a high-risk infection without undergoing chronic involution due to baseline exposure to PAMPs. One potential regulatory system that would be well adapted to tuning involution sensitivity is the microRNA (miRNA) network. MicroRNAs are small, noncoding RNAs that modulate the production of protein from mRNA through destabilization of the mRNA and inhibition of translation. In monocytes and dendritic cells, miRNA can tightly regulate the signaling resulting from exposure to PAMPs. The miRNA miR-155 is a positive regulator of Toll-like receptor signaling and downregulates the signaling inhibitor SOCS1 and inositol polyphosphate phosphatase SHIP-1 to enhance Toll-like

[1]VIB, Leuven, Belgium. [2]Center for Human Genetics, University of Leuven, Leuven, Belgium. [3]Autoimmune Genetics Laboratory, University of Leuven, Leuven, Belgium. [4]Cambridge Institute for Medical Research and Department of Medicine, University of Cambridge, Cambridge, UK. [5]Developmental Immunology, German Cancer Research Center, Heidelberg, Germany. [6]Pediatric Immunology, University of Basel, Basel, Switzerland. [7]Laboratory of Immunobiology, Rega Institute, University of Leuven, Leuven, Belgium. [8]Molecular Genetics of Cancer, The Walter and Eliza Hall Institute of Medical Research, Melbourne, Australia. [9]These authors contributed equally to this work. Correspondence should be addressed to A.L. (adrian.liston@vib.be) or J.D. (james.dooley@vib-kuleuven.be).

Received 5 October; accepted 21 November; published online 18 December 2011; doi:10.1038/ni.2193

receptor signaling[12,13]. The miRNAs miR-146a, miR-147, miR-125b, miR-21 and let-7e, in contrast, are all negative regulators of Toll-like receptor signaling and diminish the sensitivity of cells to PAMPs[14–17]. These miRNAs have a complex regulatory system, with both ligand-dependent enhancement and suppression[18]. As well as modulating the Toll-like receptor signaling pathway, miRNA-146 is also involved in the RNA helicase RIG-I antiviral pathway, diminishing the amount of the ubiquitin ligase TRAF6 and the kinases IRAK1 and IRAK2 and hence modulating IFN-α production[19]. Therefore, miRNAs are putative regulators of PAMP signaling in thymic epithelium.

To assess the function of miRNA regulation in thymic function and involution, we generated mice with thymic epithelial cell–specific deletion of Dicer, the key miRNA-biogenesis protein. We found that thymic epithelial cells were exquisitely sensitive to loss of the miRNA network, as excision of Dicer drove progressive degeneration of thymic architecture and function, altering T cell differentiation and peripheral tolerance. In addition to the disruption of thymic architecture, Dicer-deficient thymic epithelium became hypersensitive to molecular involution signals, which allowed constitutive or suboptimal amounts of pathogen-related signals to drive premature and chronic thymic involution. This heightened sensitivity was replicated in mice deficient in the miR-29a cluster (miR-29a–miR-29b-1) and was associated with loss of miR-29a-dependent regulation of IFNAR1. Loss of the miR-29a cluster resulted in IFNAR1-dependent hypersensitivity to pathogen-related signals and hyperactivity of the IFNAR1 signaling pathway. These results indicate that the miRNA network, and miR-29a in particular, is the key threshold modulator of the thymic epithelial cell response to peripheral PAMP signals.

RESULTS

Thymic architecture maintained by miRNA

To determine the function of the miRNA network in thymic epithelial cells, we used mice with a *Foxn1* locus (which encodes a highly specialized regulator of thymic epithelial cell differentiation) containing sequence encoding Cre recombinase knocked into its 3′ untranslated region (*Foxn1*^{Cre}), which produces Cre with high specific activity in thymic epithelial cell precursors[20], crossed to mice with *lox*P-flanked alleles of Dicer (*Dicer1*$^{fl/fl}$; called '*Dicer*$^{fl/fl}$' here)[21]. Histological examination of epithelial architecture in the thymus of *Foxn1*^{Cre}*Dicer*$^{fl/fl}$ mice demonstrated a progressive disruption of thymic architecture. *Dicer*-sufficient siblings (*Foxn1*$^{+/+}$*Dicer*$^{fl/fl}$ mice; called 'wild-type mice' here) typically had an even distribution of keratin 8–positive epithelial cells in the cortex and keratin 14–positive epithelial cells in the medulla, with relatively few changes in structure during development, beyond expansion of the medulla during the first weeks after birth (**Fig. 1a**). *Foxn1*^{Cre}*Dicer*$^{fl/fl}$ mice developed normal thymic architecture, with the presence of a discrete cortex and medulla at birth (**Fig. 1a**). By 1 week of age, however, disorganization of thymic structure became apparent, with the loss of homogeneity in keratin 14 expression and the appearance of regions lacking keratin 14 expression in the medulla (**Fig. 1a**). Those keratin 14–negative zones also lacked expression of other epithelial markers (**Supplementary Fig. 1**), which suggested the presence of epithelial voids in the medulla. By 3 weeks of age, large epithelial voids had also opened up in the cortex and the medullary epithelium was almost absent. These architectural changes were not present in *Foxn1*^{Cre}*Dicer*$^{+/+}$ mice (**Supplementary Fig. 2**) and were thus due to thymic epithelial cell–specific excision of *Dicer* rather than any cytotoxicity effect of Cre. The heightened sensitivity of medullary epithelium to architectural degradation was reflected in the cellular composition of the epithelial compartment, as measured by flow cytometry (**Fig. 1b**), whereby the fraction of medullary epithelium was much lower than that of the cortical epithelium in Dicer-deficient mice; this created a bias of ~25:1 in the ratio of recoverable cortical epithelium to medullary epithelium in *Foxn1*^{Cre}*Dicer*$^{fl/fl}$ mice, compared with the normal ratio of ~1:1 in wild-type mice (**Fig. 1c**).

The progressive loss of epithelium from the thymus in *Foxn1*^{Cre}*Dicer*$^{fl/fl}$ mice suggested a role for the miRNA network in preventing apoptosis of epithelial cells, with medullary epithelium showing heightened sensitivity to miRNA loss. In direct support of a model of the generation of epithelial voids by more apoptosis, costaining of keratin 8 and activated caspase-3 demonstrated the presence of apoptotic epithelial cells along the boundary of the epithelial voids in Dicer-deficient mice only (**Fig. 2a**). By staining for activated caspase-3, we found significantly more apoptotic epithelium in *Foxn1*^{Cre}*Dicer*$^{fl/fl}$ mice, especially in the medullary compartment (**Fig. 2b**). Despite the greater apoptosis in Dicer-deficient epithelium, we found no evidence for selection of Dicer-sufficient clones, with *Dicer* mRNA absent from purified thymic epithelium (**Supplementary Fig. 3**). Corresponding with the higher rate of apoptosis, epithelial markers indicative of specialized or terminal lineages, such as UEA, Aire, CDR1, claudin 3 and claudin 4, had lower expression from birth (**Supplementary Figs. 1** and **4** and data not shown). In contrast, immature epithelium seemed to be more

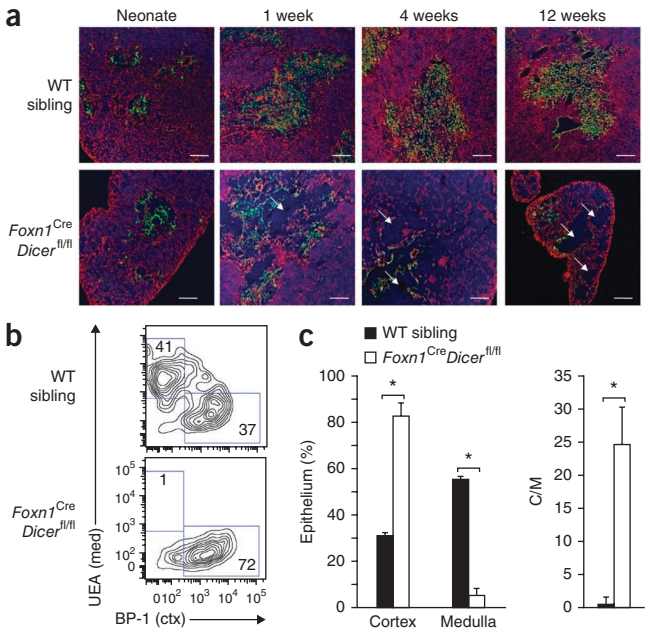

Figure 1 Loss of miRNA in the thymic epithelium results in progressive loss of thymic architecture. (**a**) Immunofluorescence staining of thymi from *Foxn1*^{Cre}*Dicer*$^{fl/fl}$ mice and their wild-type (WT) siblings assessed at birth (Neonate) and at 1, 4 and 12 weeks of age: red, keratin 8 (cortex); green, keratin 14 (medulla); blue, DNA-intercalating dye DAPI (nuclei). Arrows indicate epithelial voids. Scale bars, 100 μm. (**b**) Frequency of cortical epithelium (ctx; BP-1$^+$UEA$^-$) and medullary epithelium (med; BP-1$^-$UEA$^+$) in thymi from 12-week-old wild-type and *Foxn1*^{Cre}*Dicer*$^{fl/fl}$ mice, measured by flow cytometry and gated on CD45$^-$G8.8$^+$ epithelium. Numbers in outlined areas indicate percent UEA$^+$BP-1$^-$ cells (top left) or UEA$^-$BP-1$^+$ cells (bottom right). (**c**) Proportion of cortical and medullary epithelium (left) and cortical/medullary ratio (C/M; right) in wild-type mice ($n = 5$) and *Foxn1*^{Cre}*Dicer*$^{fl/fl}$ mice ($n = 6$), analyzed as in **b**. $^*P < 0.001$ (*t*-test). Data are representative of five experiments (**a**,**b**) or are pooled from five experiments (**c**; average and s.d.).

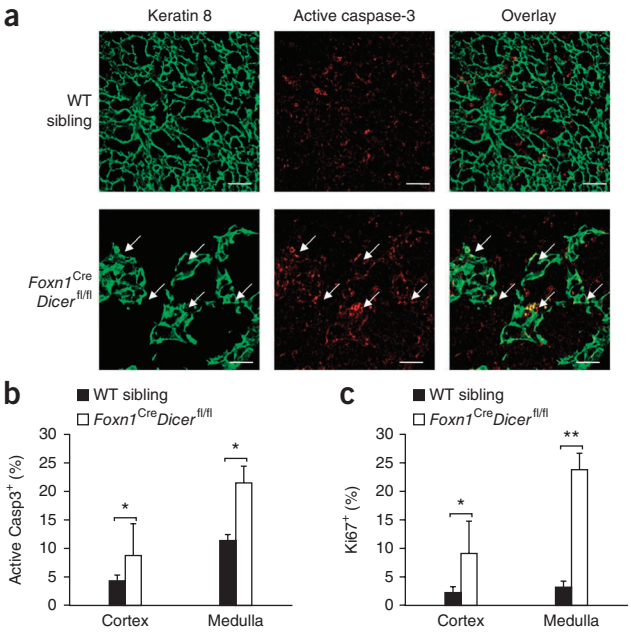

Figure 2 Enhanced apoptosis of the medullary thymic epithelium in the absence of miRNA. (**a**) Immunofluorescence staining of thymi from 12-week-old *Foxn1*^{Cre}*Dicer*$^{fl/fl}$ mice and their wild-type siblings. Green, keratin 8 (left); red, active caspase-3 (center); yellow, overlay (right). Arrows indicate apoptotic epithelial cells. Scale bars, 50 μm. (**b**,**c**) Proportion of apoptotic cells (cells with activate caspase-3 (Casp3$^+$); **b**) and frequency of proliferating cells (Ki67$^+$ cells; **c**) in the cortical (BP-1$^+$UEA$^-$) and medullary (BP-1$^-$UEA$^+$) epithelium of 12-week-old wild-type mice ($n = 4$) and their *Foxn1*^{Cre}*Dicer*$^{fl/fl}$ siblings ($n = 5$), assessed by flow cytometry in **b**. (**c**) $^*P < 0.05$ and $^{**}P < 0.001$ (*t*-test). Data are representative of five experiments (**a**) or are pooled from five experiments (**b**,**c**; average and s.d.).

abundant, with more clusters positive for keratin 5 and keratin 8 and more epithelium positive for the marker p63 (**Supplementary Fig. 4**). The greater proliferation may have been in direct response to the higher rate of apoptosis, with a higher percentage of epithelial cells expressing the proliferation marker Ki67, especially in the medullary compartment (**Fig. 2c**). More epithelial turnover, with enhanced apoptosis and more compensatory proliferation, would account for the skewing of epithelium toward relatively immature stages, although the possibility of an additional block in epithelial differentiation cannot be excluded.

Given the progressive disintegration of the thymic architecture in the absence of Dicer, we assessed whether miRNA contributed to the ability of the epithelium to support thymocyte differentiation. Despite the large changes in architecture, T cell differentiation remained notably robust. Early T cell differentiation through rearrangement of the T cell antigen receptor and β-selection was intact, with no change in the CD4$^-$CD8$^-$ (double-negative) or CD4$^+$CD8$^+$ (double-positive) thymocyte populations (**Supplementary Table 1** and **Supplementary Fig. 5**). At the neonate stage, positive selection was also unmodified, with relatively normal ratio of double-positive cells to CD4$^+$ or CD8$^+$ single-positive cells (**Fig. 3a**,**b**). Only after the development of large epithelial voids in the thymic cortex at 3 weeks of age did we observe notable defects in positive selection, with fewer CD3$^+$CD69$^+$ CD4$^+$CD8$^+$ double-positive thymocytes after positive selection (**Supplementary Table 1** and **Supplementary Fig. 5**) and CD4$^+$ or CD8$^+$ single-positive thymocytes (**Fig. 3a**,**b** and **Supplementary Fig. 5**). Functionally, the lower thymic output resulted in a net lower abundance of CD4$^+$ T cells and CD8$^+$ T cells in the periphery (**Supplementary Fig. 6a**,**b**). The combined effects of less T cell production and an almost complete loss of medullary thymic epithelial cells (**Fig. 1c**), including Aire-expressing cells (**Supplementary Fig. 4**), produced complex effects on autoimmune susceptibility, with *Foxn1*^{Cre}*Dicer*$^{fl/fl}$ mice simultaneously demonstrating a greater susceptibility to collagen-induced arthritis and a lower severity of disease (**Supplementary Fig. 6c–e** and **Supplementary Table 2**).

As the phenomena noted above could have been due to fewer interactions with the epithelium, we investigated the cellular composition of the epithelial voids further. Although epithelial voids showed an absence of thymic epithelium, they were not acellular but had thymocytes present in the cortical voids (**Fig. 3c**). The distribution of dendritic cells and vascularization of epithelial voids was largely normal, whereas fibroblasts were absent from cortical voids (**Supplementary Fig. 7**). The frequent distribution of F4/80$^+$ macrophages along the boundary of the epithelial voids (**Supplementary Fig. 7**) further supported a model of enhanced epithelial cell death in the region. An unusual feature common to the epithelial voids was the presence of dense foci of CD19$^+$ B cells, which resulted in an expansion in the total number of B cells in the thymus (**Fig. 3d**,**e**). These B cells may have represented aberrant migration into the thymus or autochthonous production from thymocyte precursors in the absence of epithelial signals. Overall, these results suggested that the Dicer-deficient

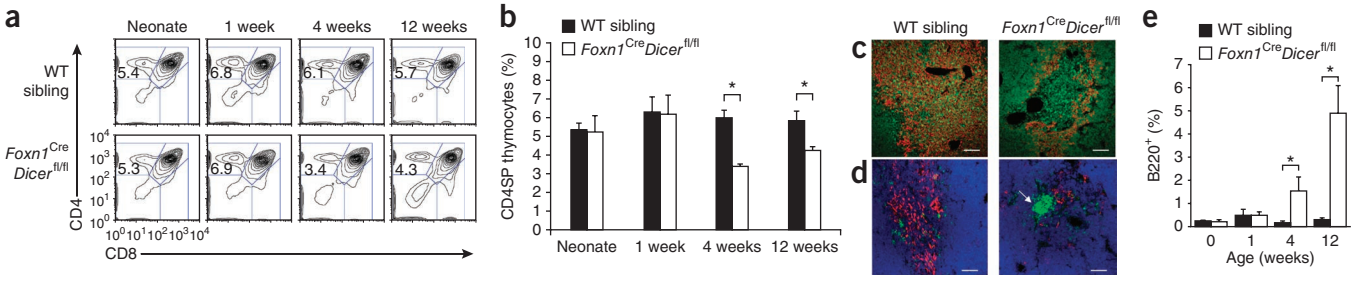

Figure 3 Progressive decay in thymocyte differentiation associated with the presence of epithelial voids in Dicer-deficient mice. (**a**) Flow cytometry of thymocytes from wild-type and *Foxn1*^{Cre}*Dicer*$^{fl/fl}$ thymi. Numbers in outlined areas indicate percent CD4$^+$CD8$^-$ (single-positive) cells. (**b**) Frequency of CD4$^+$ single-positive (CD4SP) thymocytes in mice analyzed as in **a** ($n = 2$–5 mice per group). (**c**,**d**) Immunofluorescence staining of thymi from 4-week-old *Foxn1*^{Cre}*Dicer*$^{fl/fl}$ mice and their wild-type siblings: red, keratin 14 (**c**,**d**); green, CD4 (**c**) or CD19 (**d**); blue, DAPI (**d**). In **d**, 62% of epithelial voids ($n = 53$) have CD19 foci. Scale bars, 100 μm. (**e**) Frequency of B cells in thymi from wild-type and *Foxn1*^{Cre}*Dicer*$^{fl/fl}$ siblings ($n = 2$–5 per group), assessed by flow cytometry. $^*P < 0.05$ (*t*-test). Data are representative of six (**a**) or three (**c**,**d**) experiments or are pooled from five experiments (**b**,**e**; average and s.d.).

neonatal thymus had preserved function, but that progressive defects in thymocyte differentiation and selection processes developed in line with the altered architecture.

miRNAs prevent pathogen-associated thymic involution

Coincident with the thymic architectural changes, Dicer deficiency in the thymic epithelium caused premature thymic involution. Although thymus size in *Foxn1*^{Cre}*Dicer*$^{fl/fl}$ mice was normal at birth and the thymus grew to nearly normal sizes by 4 weeks of age, after that age it began to rapidly involute, dropping by 90% at 12 weeks (**Fig. 4a**). To determine if miRNA protects against thymic involution by modulating the sensitivity of the thymic epithelium to sex hormones, we surgically castrated *Foxn1*^{Cre}*Dicer*$^{fl/fl}$ mice and their wild-type siblings at 7 weeks of age. Although castrated wild-type and Dicer-deficient mice demonstrated a gain in thymic cellularity at 12 weeks (**Fig. 4b**), the difference between the two conditions was not eliminated, which indicated that the loss of thymic epithelial miRNA did not affect sensitivity to a sex-hormone signal.

The second main pathway involved in thymic involution is the IFN-α-mediated pathway. By a 'bioinformatics discovery' approach, IFNAR1 was the only component of the IFN-α signaling pathway with higher expression in Dicer-deficient thymic epithelium (S.Z. and G.A.H., data not shown). To determine if miRNA regulates sensitivity of thymic epithelial cells to IFN-α signaling, we purified cortical thymic epithelium (BP-1$^+$UEA$^-$) and medullary thymic epithelium (BP-1$^-$UEA$^+$) from wild-type and Dicer-deficient mice. In the thymus of Dicer-deficient mice, *Ifnar1* mRNA was upregulated about tenfold in the cortex and about fivefold in the medulla, relative to *Ifnar1* mRNA expression in the same cell populations from wild-type mice (**Fig. 4c**). IFNAR1 expression on the thymic stroma is critical for poly(I:C)-mediated thymic involution[4], which suggests that Dicer deficiency may drive inappropriate thymic involution through enhanced sensitivity of thymic epithelial cells to PAMP signals. To directly test that hypothesis, we 'titrated' poly(I:C) exposure in wild-type mice to determine the concentration of poly(I:C) unable to induce thymic involution. Doses of 250 μg per mouse and above induced thymic involution, whereas doses of 200 μg per mouse and below were unable to drive involution in wild-type mice (**Fig. 4d**). Dicer-deficient mice, unlike wild-type mice, were hypersensitive to a low dose of poly(I:C) and underwent rapid thymic involution when exposed to suboptimal doses of poly(I:C) (**Fig. 4e**). These data demonstrated that the thymic epithelial miRNA network was important for protecting the thymus from inappropriate involution at low concentrations of PAMPs.

The miR-29a cluster controls thymic involution

A likely miRNA candidate for hypersensitivity to PAMP-mediated thymic involution was miR-29a. Among the miRNAs expressed in the thymic epithelium (S.Z. and G.A.H., data not shown), miR-29a was the miRNA with the highest expression predicted to have multiple interactions with *Ifnar1* mRNA (ref. 22). To determine whether miR-29a targeted *Ifnar1* as predicted, we cloned the 3′ untranslated region of *Ifnar1* into the 3′ region of a luciferase reporter gene. The addition of a miR-29a mimic to HeLa-M human cervical cancer cells resulted in the destabilization of mRNA containing the *Ifnar* 3′ UTR region, but the addition of a mimic with scrambled sequence did not (**Fig. 5a**), which demonstrated the specific ability of miR-29a to destabilize mRNA containing that region. Because of the potential redundancy in function of miR-29a, miR-29b and miR-29c, we assessed the expression of all three miRNAs by *in situ* hybridization. In the brain, all three miRNAs had high expression (**Fig. 5b**); however, in the thymus, we detected only miR-29a in substantial amounts (**Fig. 5b**). The detection of only miR-29a and not miR-29b in the thymus, despite cotranscription from the bicistronic miR-29a cluster, suggested independent regulation of expression, a feature described before for the miR-29a locus, with a 3′ hexanucleotide sequence in miR-29b driving nuclear localization and accelerated turnover during the nonmitotic portions of the cell cycle[23]. The *in situ* data indicating lower expression of miR-29b than miR-29a in thymic epithelial cells was supported by microarray analysis, whereby miR-29a expression was high in the cortex and medulla but miR-29b expression was low to undetectable (S.Z. and G.A.H., data not shown), and by quantitative PCR analysis, whereby miR-29a expression was high but miR-29b expression was undetectable in half the samples and very low in others (**Supplementary Fig. 8**).

To assess the function of miR-29a in the thymus, we generated mice with targeted deletion of the miR-29a–miR-29b-1 locus (called 'miR-29a-deficient mice' here). We removed a region of about 1.7 kilobases spanning the entire miR-29a–miR-29b-1 cluster precursor sequence by homologous recombination (**Supplementary Fig. 9a**) and confirmed the loss of miR-29a–miR-29b-1 by Southern blot analysis (**Supplementary Fig. 9b**).

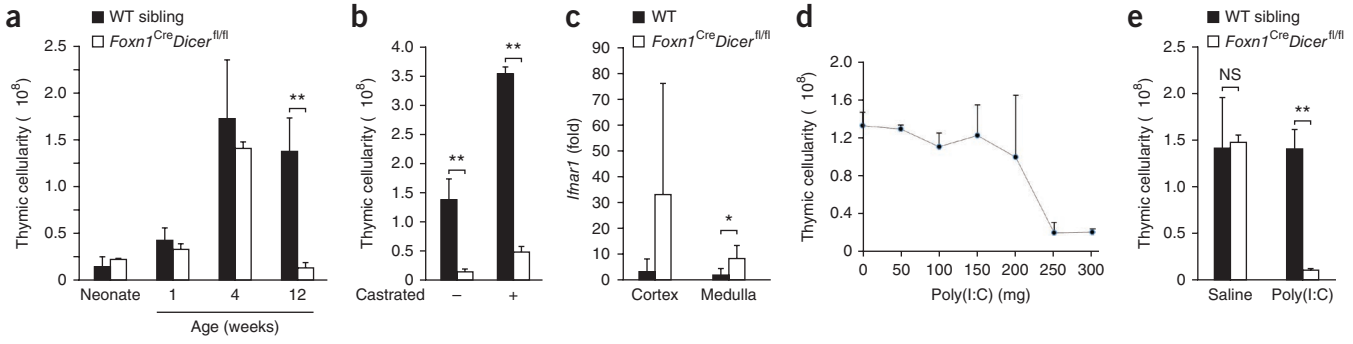

Figure 4 Thymic epithelial defects in the miRNA network result in hypersensitivity to IFN-α and premature thymic involution. (**a**) Thymic cellularity of wild-type and *Foxn1*^{Cre}*Dicer*$^{fl/fl}$ mice (n = 3–17 per group) assessed at birth and 1, 4 and 12 weeks of age. (**b**) Thymic cellularity in wild-type and *Foxn1*^{Cre}*Dicer*$^{fl/fl}$ mice (n = 3–7 per group) left intact (–) or surgically castrated (+) at 7 weeks of age, assessed at 12 weeks. (**c**) *Ifnar1* mRNA expression in cortical (BP-1$^+$UEA$^-$) and medullary (BP-1$^-$UEA$^+$) thymic epithelium from 6- to 8-week-old wild-type mice (n = 5) and *Foxn1*^{Cre}*Dicer*$^{fl/fl}$ mice (n = 4), presented relative to values for wild-type cortex. (**d**) Thymic cellularity of wild-type mice injected with 0–300 μg poly(I:C) at 4 weeks of age (n = 3–8 per group). (**e**) Thymic cellularity of wild-type and *Foxn1*^{Cre}*Dicer*$^{fl/fl}$ mice (n = 3–5 per group) treated with saline or 150 μg poly(I:C) at 4 weeks of age. $^*P < 0.05$ and $^{**}P < 0.0001$ (t-test); NS, nonsignificant. Data are pooled from five experiments (**a**), one experiment (**b**) or three experiments (**c**–**e**; error bars, s.d.).

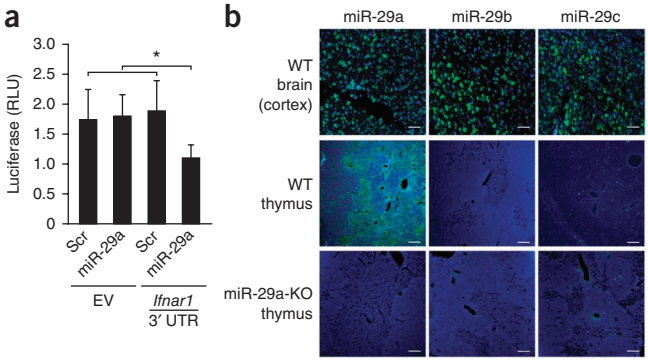

Figure 5 *Ifnar1* is a direct target of miR-29a. (**a**) Luciferase expression in HeLa-M cells ($n = 5$ replicates per group) transfected with empty renilla luciferase reporter plasmid (EV) or plasmid containing the *Ifnar1* 3′ untranslated region (*Ifnar1* 3′ UTR) and treated with the miR-29a mimic or a mimic with scrambled sequence (Scr), presented as relative luciferase units (RLU) relative to firefly luciferase. $^*P < 0.05$ (*t*-test). (**b**) *In situ* hybridization of miR-29a, miR-29b and miR-29c in the brains of wild-type mice and thymi of wild-type or miR-29a-deficient mice (miR-29a-KO): green, miRNA probe; blue, DAPI. Scale bars, 100 μm. Data are representative of three independent experiments (**a**; error bars, s.d.) or two experiments (**b**).

In situ hybridization of miR-29a-deficient thymus demonstrated complete loss of miR-29a expression without substantial compensatory upregulation of miR-29b or miR-29c (**Fig. 5b**). Our initial characterization of these mice indicated no major developmental defects, showing birth at a normal Mendelian ratio and no noticeable abnormalities in major organs such as the brain (**Supplementary Fig. 10** and **Supplementary Table 3**).

Analysis of miR-29a-deficient thymus demonstrated that the thymic architecture and thymic involution phenotypes of the Dicer-deficient mice segregated in the miR-29a-deficient mouse. Unlike $Foxn1^{Cre}Dicer^{fl/fl}$ mice, miR-29a-deficient mice demonstrated no major changes to thymic architecture, with normal development of the cortical and medullary thymic epithelial populations and no progressive decay or formation of epithelial voids (**Fig. 6** and **Supplementary Figs. 11** and **12**). Likewise, thymic function seemed intact, with normal differentiation of thymocytes and peripheral T cells (**Supplementary Fig. 13** and **Supplementary Table 4**). However, miR-29a-deficient mice did undergo premature thymic involution after 4 weeks of age (**Fig. 6c**) at a degree indistinguishable from that of $Foxn1^{Cre}Dicer^{fl/fl}$ mice (**Supplementary Fig. 14a,b**). As with $Foxn1^{Cre}Dicer^{fl/fl}$ mice, this premature involution was independent of the amount of sex hormones, as it was not reversed by chemical castration (**Supplementary Fig. 14c**). Unlike the loss of Dicer in $Foxn1^{Cre}Dicer^{fl/fl}$ mice, loss of miR-29a was not restricted to the thymic epithelium, which raised the possibility that the same phenotype was being generated through alterations in other anatomical compartments, such as T cell precursors in the bone marrow. We therefore used bone marrow chimeras and thymic transplants to test compartmentalization. Wild-type recipients of either miR-29a-deficient or wild-type bone marrow had thymi of normal size. In contrast, miR-29a-deficient recipients of either miR-29a-deficient or wild-type bone marrow had much smaller (90%) thymi (**Fig. 6d**). When we transplanted thymi from neonatal miR-29a-deficient mice or their wild-type siblings into wild-type hosts, wild-type thymi grafted well and grew in size, whereas miR-29a-deficient thymi involuted (**Fig. 6e**). These results conclusively demonstrated that the premature thymic involution observed in miR-29a-deficient mice was due to loss of miR-29a in the thymic epithelial compartment and was not secondary to changes occurring in other cell types.

The miR-29a cluster suppresses *Ifnar1*

To determine whether the inappropriate thymic involution in the miR-29a-deficient mouse was due to PAMP hypersensitivity, we measured *Ifnar1* mRNA in purified cortical and medullary epithelium in the preinvolution thymus. As befitting a true direct target, *Ifnar1* expression was about eightfold higher in miR-29a-deficient epithelium than in wild-type epithelium (**Fig. 7a**), a scale similar to that observed in Dicer-deficient epithelium. The higher *Ifnar1* mRNA expression was greater in the medulla after thymic involution (**Supplementary Fig. 15**), suggestive of initiation of a positive feedback loop. To directly assess whether this heightened expression recapitulated the Dicer-deficiency phenotype of hypersensitivity to PAMP signals, we exposed wild-type and miR-29a-deficient mice to suboptimal amounts of poly(I:C). Unlike wild-type mice, but like Dicer-deficient mice, miR-29a-deficient mice were hypersensitive to a low dose of poly(I:C) and underwent rapid thymic involution (**Fig. 7**). This hypersensitivity was dependent on IFNAR1, as coinjection of antibody to IFNAR1 (anti-IFNAR1) restored ~60% of thymic cellularity, but coinjection of isotype-matched control antibody did not, in line with

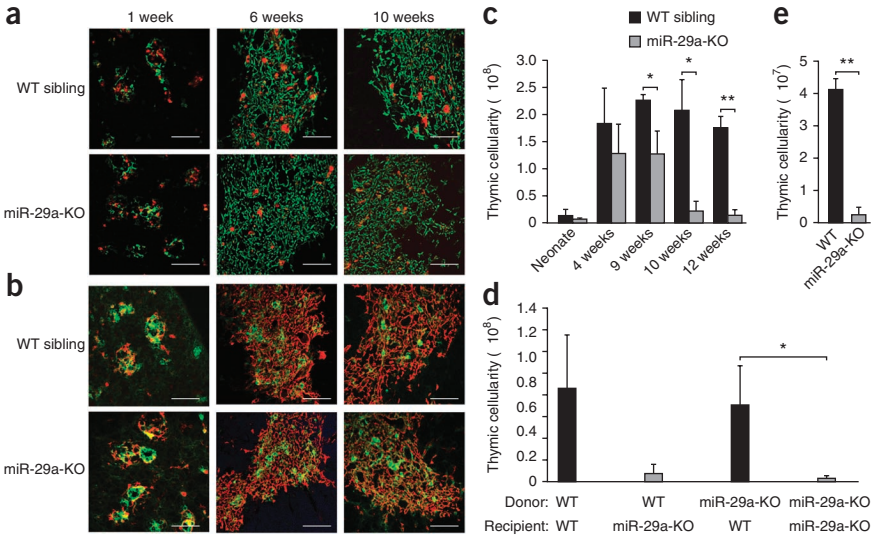

Figure 6 Thymic involution and architectural alterations segregate in miR-29a-deficient mice. (**a**,**b**) Immunofluorescence staining of thymi from wild-type and miR-29a-deficient mice assessed at 1, 6 and 10 weeks of age: red, UEA (**a**) or keratin 14 (**b**); green, keratin 14 (**a**) or G8.8 (EPCAM; **b**). Scale bars, 100 μm. (**c**) Thymic cellularity of wild-type and miR-29a-deficient mice ($n = 2$–7 per group) at birth and at 4, 9, 10 and 12 weeks of age. (**d**) Thymic cellularity of chimeras generated by the transfer of wild-type or miR-29a-deficient bone marrow into wild-type or miR-29a-deficient recipient mice ($n = 4$–13 per group). (**e**) Thymic cellularity of wild-type mice given transplantation of wild-type thymus ($n = 3$) or miR-29a-deficient thymus ($n = 4$), assessed at 6 weeks after transplantation. $^*P < 0.05$ and $^{**}P < 0.0001$ (*t*-test). Data are representative of five experiments (**a**,**b**) or are pooled from five experiments (**c**) or three experiments (**d**,**e**; error bars (**c**–**e**), s.d.).

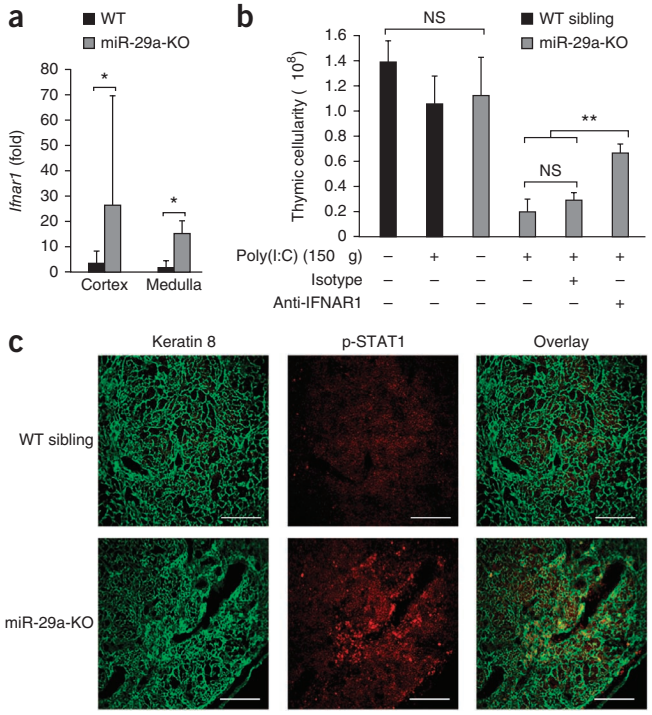

Figure 7 Thymic epithelial defects in miR-29a result in PAMP hypersensitivity and inappropriate thymic involution. (**a**) *Ifnar1* mRNA expression in cortical (BP-1$^+$UEA$^-$) and medullary (BP-1$^-$UEA$^+$) thymic epithelium from 6- to 8-week-old wild-type mice ($n = 5$) and miR-29a-deficient mice ($n = 3$), presented relative to values for wild-type cortex. (**b**) Thymic cellularity of 4-week-old wild-type and miR-29a-deficient mice ($n = 3$–10 per group) left untreated or treated with 150 μg poly(I:C) at 4 weeks, with or without coinjection of anti-IFNAR1 or isotype-matched control antibody (Isotype). (**c**) Immunofluorescence staining of thymi from 12-week-old wild-type and miR-29a-deficient mice: green, keratin 8 (left); red, phosphorylated (p-) STAT1 (center); yellow, colocalization (right). Scale bars, 100 μm. $^*P < 0.05$ and $^{**}P < 0.0001$ (*t*-test). NS, not significant. Data are pooled from three experiments (**a**,**b**) or are representative of two experiments (**c**; error bars (**a**,**b**), s.d.).

the neutralization capacity of ~60% for this antibody[24]. The ability of miR-29a-deficient mice to recover from poly(I:C) seemed intact, with ~50% cellular recovery 10 d after treatment (**Supplementary Fig. 16**). Even when not treated with a low dose of poly(I:C), by 12 weeks of age miR-29a-deficient mice had more phosphorylation of STAT1, the direct downstream target of IFNAR1, evidence that the greater abundance of *Ifnar1* mRNA had a biologically relevant effect. Together these results demonstrated that loss of miR-29a in the thymic stroma resulted in premature thymic involution and hypersensitivity to pathogen-associated signals, indistinguishable from complete loss of the miRNA network in thymic epithelium.

DISCUSSION

The role of miRNA in the adaptive immune system has been investigated through systematic removal of the miRNA network in T cells[25,26], B cells[27] and key accessory cell lineages such as dendritic cells[28]. Although many functions of the adaptive immune system seem to be independent of the miRNA network, several key aspects are under tight miRNA-mediated control, including stability of the regulatory T cell lineage[29], immunoglobulin repertoire generation[27] and PAMP responsiveness[28]. One of the main accessory cell types in the adaptive immune system whose miRNA function has not yet been profiled is the thymic epithelial cell. Here we used conditional deletion of *Dicer* to show that loss of the miRNA network in thymic epithelial cells led to decay of the epithelial architecture, less thymocyte positive selection, an enhanced B cell presence, greater susceptibility to induced autoimmunity and inappropriate chronic thymic involution. This diverse array of phenotypes can be explained by the following two distinct cellular processes: first, an miR-29a-independent increase in epithelial cell apoptosis, which gives a parsimonious account for most of the phenotypes observed; and second, miR-29a-dependent sensitivity to thymic involution.

The root driver of the miR-29a-independent phenotypes was probably changes in thymic architecture. The progressive loss of thymic epithelium was the first phenotype to appear, chronologically, with epithelial voids apparent by 1 week of age. It is likely that these epithelial voids were formed by enhanced rates of apoptosis in Dicer-deficient epithelium, with the enhanced epithelial cell proliferation and immature cells suggestive of a compensatory process. Two separate explanations can be postulated for why the enhanced apoptosis resulted in epithelial voids rather than a generalized lower epithelial density across the thymus. First, the death may have been synchronized among expanses of the thymus populated by clonal epithelial cells[30], where intrinsic sensitivity could create a large void through synchronous death. Second, the epithelial void may have progressively formed because of extrinsic effects resulting from localization along the void boundary. As thymic epithelial cells are very much reliant on the three-dimensional network[31,32], loss of interactions at the edge of the void may be sufficient to elicit apoptosis. Alternatively, proliferation of cells at the edge of the void in compensation may place them at a greater risk of apoptosis, as Dicer-deficient cells are especially vulnerable to apoptosis during proliferation[33]. The presence of apoptotic epithelial cells along the void perimeter may support the second explanation but does not rule out the first. The reason for the chronological primacy in void formation in the medulla remains an open question, but it may reflect enhanced sensitivity to one of the models described above.

The remaining thymic phenotypes can be explained as secondary effects resulting from the primary decay in thymic architecture. We did not observe the defects in positive selection and the greater B cell numbers in mice before 4 weeks of age, which suggested that these changes resulted not from abnormal regulation of key epithelial proteins but instead from the 'anatomical traps' formed by epithelial cell decay. Early thymocytes precursors that enter the thymus and find themselves in the absence of expression of ligand for the receptor Notch by thymic epithelial cells may default into B cell differentiation[34,35]. Likewise, double-positive thymocytes that migrate into epithelial cell voids would have less interaction with cortical epithelial cells, which would probably result in less positive selection. It is notable that the defect in positive selection is observed solely in the lineage differentiating into CD4$^+$ single-positive cells, as CD8$^+$ single-positive selection can occur with less efficiency through interaction with non-epithelial cells[36]. The finding of greater susceptibility of Dicer-deficient mice to autoimmunity was also supported by the 'anatomical trap' model, as single-positive thymocytes in Dicer-deficient mice have very low exposure to medullary epithelium and Aire$^+$ epithelial cells for efficient negative selection. The progressive decay observed here is probably not amenable to delineation to a single miRNA or mRNA target. Although individual miRNAs have been shown to induce apoptosis[18] or suppress apoptosis[37], the observation of enhanced apoptosis in Dicer-deficient cell types of diverse origin[27,38,39] suggests that this is an emergent feature of regulatory disruption of the whole-network deletion achieved by excision of *Dicer*.

In contrast, the most striking feature of the Dicer-deficient thymus, inappropriate chronic involution, can be accounted for by a single

miRNA-mRNA interaction. It is notable that both Dicer-deficient and miR-29a-deficient thymi developed to a normal size at birth and expanded during growth to 4 weeks before collapsing in size between 9 and 12 weeks of age. That observation indicates that the phenomenon was involution and not a failure in thymic growth. The inappropriate involution caused by loss of miR-29a expression can be explained by the loss of tight regulation of IFNAR1 expression. We demonstrated here that *ifnar1* was a true target of miR-29a and that expression of IFNAR1 was upregulated in thymic epithelium after the loss of Dicer or miR-29a. Furthermore, IFNAR1 upregulation enhanced the sensitivity of the thymic epithelium to PAMP signals, driving thymic involution at suboptimal PAMP exposure. The spontaneous thymic involution in older miR-29a-deficient mice was accompanied by activation of STAT1, and thus greater sensitivity to baseline IFN-α is the parsimonious explanation for the observed chronic involution. In this model, miR-29a has a key role in the thymic epithelium in limiting IFNAR1 expression and hence diminishing the threshold at which thymic epithelial cells become triggered to undergo involution. In the absence of epithelial miRNA, baseline PAMP exposure is sufficient to trigger the chronic involution observed. In contrast, in the presence of epithelial miRNA, the thymus is buffered against small amounts of IFN-α, which permits involution to be triggered only after an adequate infectious trigger. The published observation that exposure to both IFN-α and PAMPs drives the downregulation of Dicer[40] raises the possibility that positive feedback loops may be induced by pathogen exposure, whereby the amounts of IFN-α sufficient to drive Dicer downregulation result in upregulation of IFNAR1, initiating the involution cascade.

METHODS

Methods and any associated references are available in the online version of the paper at http://www.nature.com/natureimmunology/.

Note: Supplementary information is available on the Nature Immunology website.

ACKNOWLEDGMENTS

We thank A. Tarakhovsky (Rockefeller University) for *Dicer*^{fl} mice; N. Manley (University of Georgia) for *Foxn1*^{Cre} mice; A. Farr (University of Washington) for hybridomas; S. Schonefeldt for mouse colony support and D. Anz for discussions. Supported by the VIB and Fonds Wetenschappelijk Onderzoek (A.L.), Methusalem financing (KULeuven and Flemish government), European Research Council (B.D.S.), Agentschap voor Innovtie door Wetenschap en Technologie (W.P.), the Australian National Health and Medical Research Council (D.H.D.G.), the European Union consortium "Tolerage" and the Deutsches Krebsforschungszentrum (B.K.).

AUTHOR CONTRIBUTIONS

A.S.P., J.D., M.A.L., W.P. and O.U. did the experiments; B.K., S.Z., G.A.H. and D.H.D.G. shared data for study design; J.D., P.M., B.D.S. and A.L. designed the study; J.D. and A.L. wrote the manuscript; and all authors read and approved the manuscript.

COMPETING FINANCIAL INTERESTS

The authors declare no competing financial interests.

Published online at http://www.nature.com/natureimmunology/.
Reprints and permissions information is available online at http://www.nature.com/reprints/index.html.

1. Miller, J.F. Immunological function of the thymus. *Lancet* **2**, 748–749 (1961).
2. Itoh, M. *et al.* Thymus and autoimmunity: production of CD25$^+$CD4$^+$ naturally anergic and suppressive T cells as a key function of the thymus in maintaining immunologic self-tolerance. *J. Immunol.* **162**, 5317–5326 (1999).
3. King, C.C. *et al.* Viral infection of the thymus. *J. Virol.* **66**, 3155–3160 (1992).
4. Anz, D. *et al.* Activation of melanoma differentiation-associated gene 5 causes rapid involution of the thymus. *J. Immunol.* **182**, 6044–6050 (2009).
5. Aronson, M. Hypothesis: involution of the thymus with aging–programmed and beneficial. *Thymus* **18**, 7–13 (1991).
6. Dowling, M.R. & Hodgkin, P.D. Why does the thymus involute? A selection-based hypothesis. *Trends Immunol.* **30**, 295–300 (2009).
7. Fu, Y., Paul, R.D., Wang, Y. & Lopez, D.M. Thymic involution and thymocyte phenotypic alterations induced by murine mammary adenocarcinomas. *J. Immunol.* **143**, 4300–4307 (1989).
8. Olsen, N.J., Olson, G., Viselli, S.M., Gu, X. & Kovacs, W.J. Androgen receptors in thymic epithelium modulate thymus size and thymocyte development. *Endocrinology* **142**, 1278–1283 (2001).
9. Sutherland, J.S. *et al.* Activation of thymic regeneration in mice and humans following androgen blockade. *J. Immunol.* **175**, 2741–2753 (2005).
10. Domínguez-Gerpe, L. & Rey-Mendez, M. Time-course of the murine lymphoid tissue involution during and following stressor exposure. *Life Sci.* **61**, 1019–1027 (1997).
11. Sasaki, S., Ishida, Y., Nishio, N., Ito, S. & Isobe, K. Thymic involution correlates with severe ulcerative colitis induced by oral administration of dextran sulphate sodium in C57BL/6 mice but not in BALB/c mice. *Inflammation* **31**, 319–328 (2008).
12. Rodriguez, A. *et al.* Requirement of bic/microRNA-155 for normal immune function. *Science* **316**, 608–611 (2007).
13. Martinez-Nunez, R.T., Louafi, F., Friedmann, P.S. & Sanchez-Elsner, T. MicroRNA-155 modulates the pathogen binding ability of dendritic cells (DCs) by down-regulation of DC-specific intercellular adhesion molecule-3 grabbing non-integrin (DC-SIGN). *J. Biol. Chem.* **284**, 16334–16342 (2009).
14. Taganov, K.D., Boldin, M.P., Chang, K.J. & Baltimore, D. NF-κB-dependent induction of microRNA miR-146, an inhibitor targeted to signaling proteins of innate immune responses. *Proc. Natl. Acad. Sci. USA* **103**, 12481–12486 (2006).
15. Liu, G. *et al.* miR-147, a microRNA that is induced upon Toll-like receptor stimulation, regulates murine macrophage inflammatory responses. *Proc. Natl. Acad. Sci. USA* **106**, 15819–15824 (2009).
16. Sheedy, F.J. *et al.* Negative regulation of TLR4 via targeting of the proinflammatory tumor suppressor PDCD4 by the microRNA miR-21. *Nat. Immunol.* **11**, 141–147 (2010).
17. Androulidaki, A. *et al.* The kinase Akt1 controls macrophage response to lipopolysaccharide by regulating microRNAs. *Immunity* **31**, 220–231 (2009).
18. Liston, A., Linterman, M. & Lu, L.F. MicroRNA in the adaptive immune system, in sickness and in health. *J. Clin. Immunol.* **30**, 339–346 (2010).
19. Hou, J. *et al.* MicroRNA-146a feedback inhibits RIG-I-dependent Type I IFN production in macrophages by targeting TRAF6, IRAK1, and IRAK2. *J. Immunol.* **183**, 2150–2158 (2009).
20. Liston, A. *et al.* Lack of Foxp3 function and expression in the thymic epithelium. *J. Exp. Med.* **204**, 475–480 (2007).
21. Yi, R. *et al.* Morphogenesis in skin is governed by discrete sets of differentially expressed microRNAs. *Nat. Genet.* **38**, 356–362 (2006).
22. Betel, D., Wilson, M., Gabow, A., Marks, D.S. & Sander, C. The microRNA.org resource: targets and expression. *Nucleic Acids Res.* **36**, D149–D153 (2008).
23. Hwang, H.W., Wentzel, E.A. & Mendell, J.T. A hexanucleotide element directs microRNA nuclear import. *Science* **315**, 97–100 (2007).
24. Sheehan, K.C.F. *et al.* Blocking monoclonal antibodies specific for mouse IFN-α/β receptor subunit 1 (IFNAR-1) from mice immunized by in vivo hydrodynamic transfection. *J. Interferon Cytokine Res.* **26**, 804–819 (2006).
25. Muljo, S.A. *et al.* Aberrant T cell differentiation in the absence of Dicer. *J. Exp. Med.* **202**, 261–269 (2005).
26. Cobb, B.S. *et al.* T cell lineage choice and differentiation in the absence of the RNase III enzyme Dicer. *J. Exp. Med.* **201**, 1367–1373 (2005).
27. Koralov, S.B. *et al.* Dicer ablation affects antibody diversity and cell survival in the B lymphocyte lineage. *Cell* **132**, 860–874 (2008).
28. Kuipers, H., Schnorfeil, F.M., Fehling, H.J., Bartels, H. & Brocker, T. Dicer-dependent microRNAs control maturation, function, and maintenance of Langerhans cells in vivo. *J. Immunol.* **185**, 400–409 (2010).
29. Liston, A., Lu, L.F., O'Carroll, D., Tarakhovsky, A. & Rudensky, A.Y. Dicer-dependent microRNA pathway safeguards regulatory T cell function. *J. Exp. Med.* **205**, 1993–2004 (2008).
30. Rodewald, H.R., Paul, S., Haller, C., Bluethmann, H. & Blum, C. Thymus medulla consisting of epithelial islets each derived from a single progenitor. *Nature* **414**, 763–768 (2001).
31. Sato, T. *et al.* Surface molecules essential for positive selection are retained but interfered in thymic epithelial cells after monolayer culture. *Cell. Immunol.* **211**, 71–79 (2001).
32. Flomerfelt, F.A., Kim, M.G. & Schwartz, R.H. Spatial, a gene expressed in thymic stromal cells, depends on three-dimensional thymus organization for its expression. *Genes Immun.* **1**, 391–401 (2000).
33. Fukagawa, T. *et al.* Dicer is essential for formation of the heterochromatin structure in vertebrate cells. *Nat. Cell Biol.* **6**, 784–791 (2004).
34. Anderson, G., Pongracz, J., Parnell, S. & Jenkinson, E.J. Notch ligand-bearing thymic epithelial cells initiate and sustain Notch signaling in thymocytes independently of T cell receptor signaling. *Eur. J. Immunol.* **31**, 3349–3354 (2001).
35. Wilson, A., MacDonald, H.R. & Radtke, F. Notch 1-deficient common lymphoid precursors adopt a B cell fate in the thymus. *J. Exp. Med.* **194**, 1003–1012 (2001).
36. Bix, M. & Raulet, D. Inefficient positive selection of T cells directed by haematopoietic cells. *Nature* **359**, 330–333 (1992).
37. Lu, L.F. & Liston, A. MicroRNA in the immune system, microRNA as an immune system. *Immunology* **127**, 291–298 (2009).
38. Fedeli, M. *et al.* Dicer-dependent microRNA pathway controls invariant NKT cell development. *J. Immunol.* **183**, 2506–2512 (2009).
39. Lynn, F.C. *et al.* MicroRNA expression is required for pancreatic islet cell genesis in the mouse. *Diabetes* **56**, 2938–2945 (2007).
40. Wiesen, J.L. & Tomasi, T.B. Dicer is regulated by cellular stresses and interferons. *Mol. Immunol.* **46**, 1222–1228 (2009).

ONLINE METHODS

Mice. *Foxn1*^{cre} mice[41] were intercrossed with *Dicer*^{fl} mice[21] to produce mice on the C57BL/6 background with excision of Dicer specific to thymic epithelial cells. The miR-29a-deficient mice were generated as described below. Mice were chemically castrated at 4 months of age by intramuscular injection of 0.4 mg leuprorelin acetate (Lupron), followed by analysis at 6 months of age. Mice were surgically castrated at 7 weeks of age and assessed at 12 weeks of age[9]. Bone marrow chimeras were generated by injection of bone marrow (1×10^6 cells per recipient) treated with complement (Low-Tox M Rabbit Complement; Cedarlane) into irradiated host mice (9.5 Gy). Neonatal thymus was transplantated under the kidney capsule at 6 weeks of age under sterile conditions. High-molecular-weight poly(I:C) (Invivogen) was injected intraperitoneally on days 0 and 3, with cellularity measured on day 4. In neutralization experiments, 0.75 mg anti-IFNAR1 (MAR1-5A3; Biolegend) or isotype-matched control antibody (GIR-208; Biolegend) was injected intravenously on days 0 and 3 at 1 h before treatment with poly(I:C). Histology was done by Histology Consultation Services and pathology reports were generated by BioGenetics. Mice were housed under specific pathogen–free conditions and were used in accordance with the University of Leuven Animal Ethics Committee.

Generation of miR-29a-deficient mice. Bacterial artificial chromosome clone RPCIB731L15459Q2 was used as the source for the 10.9-kilobase region surrounding the miR-29a–miR-29b-1 gene. A 1.7-kilobase region between the 5′ AfeI site and the 3′ SalI site was deleted by the introduction of a gene encoding hygromycin resistance, and the linearized pBluescript II KSM vector was transfected by electroporation into E14 129/Ola mouse embryonic stem cells. Clones that underwent homologous recombination events were identified by hygromycin selection and were screened by Southern blot analysis. Genomic DNA was digested with EcoRI, EcoRV or NcoI and was hybridized to a genomic DNA external 5′ probe (PCR product with primers 5′-ACCCTGACATTGACACAGC-3′ (forward) and 5′-AAAGGGGTCTTAGCATCCA-3′ (reverse)) and 3′probe (PCR product with primers 5′-CTAGAGCCAAGGATAGCTGTGT-3′ (forward) and 5′-CCTTCATGAGCGTGTAAGACA-3′ (reverse)) and an internal hygromycin DNA probe (PCR product with primers 5′-CAGCGAGAGCCTGACCTATTGC-3′ (forward) and 5′-CGATCCTGCAAGCTCCGGATG-3′ (reverse)). Embryonic stem cell clones were microinjected into C57BL/6 bastocysts for the generation of chimeras. The chimeras then were backcrossed to C57BL/6 mice for more than seven generations. Mice deficient in miR-29a were genotyped by PCR with primers for the wild-type band (561 base pairs; 5′-CTTAATTCTTACCTGTGGCTCCAACG-3′ (forward) and 5′-GAACTATTGCACGGACTTCACCTTCC-3′ (reverse)) and knockout band (717 base pairs; 5′-AAATGGTTCAAACGCTCCAC-3′ (forward) and 5′-CAGAAAGCGAAGGAGCAAAG -3′ (reverse)).

Arthritis induction. Collagen-induced arthritis was induced by intradermal injection of chicken collagen type II (Sigma-Aldrich) in Freund's complete adjuvant, as described[42]. Clinical severity of disease was monitored for 40 d after induction with a published scoring system[43]. Susceptibility to arthritis was assessed as the incidence of arthritis at completion, with four independent groups (two male and two female) treated as paired values in a two-tailed *t*-test. Arthritis severity among affected mice showed no substantial difference across sex or replicates; thus, groups were merged and differences in severity were tested with unpaired *t*-tests for each time point and maximum disease score.

Flow cytometry and immunofluorescence. Mice were analyzed with the following antibodies: fluorescein isothiocyanate–conjugated anti-CD69 (H1.2F3; eBioscience), anti-CD25 (IL-2Rα; p55; eBioscience), anti-IgM (11/41; eBioscience) and Ulex Europaeus Agglutinin (Vector Labs); phycoerythrin-conjugated anti-CD8 (53.6.7), anti-CD19 (1D3) and anti-BP-1 (6C3; all from eBioscience); peridinin chlorophyll protein–conjugated anti-CD3 (145-2C11; eBioscience) and anti-B220 (RA3-6B2; eBioscience); allophycocyanin-conjugated anti-Foxp3 (FJK-16s; eBioscience), anti-CD44 (1M7; eBioscience), anti-CD45 (104; eBioscience), anti-CD43 (eBioR2/60; eBioscience) and anti-Ki67 (B56; BD Pharmingen); phycoerythrin-indotricarbocyanine-conjugated anti-CD4 (RM4-5; eBioscience), anti-CD23 (B3B4; eBioscience) and anti-EPCAM (G8.8; Biolegend); biotin-conjugated antibody to active caspase-3 (550557; BD Pharmingen), followed by streptavidin–Alexa Fluor 647; and phycoerythrin–cyanine 5.5–conjugated antibody to I-A–I-E (M5/114.15.2; Biolegend). Intracellular staining was done after cells were fixed and made permeable with reagents from the eBiosciences Foxp3 staining kit.

Thymus sections were prepared and stained as described[44]. Brain tissues were fixed in 4% (vol/vol) paraformaldehyde, made permeable in 0.25% (vol/vol) Triton-X100 and blocked with 1% Blocking Reagent (Roche) in 0.2% (vol/vol) FCS. Sections were stained with monoclonal antibody to keratin 8(Troma-1; Developmental Studies Hybridoma Bank), anti-meca-32 (Meca-32; in-house supernatant), anti-CD4 (GK1.5; in-house supernatant), anti-CD8 (2.43; in-house supernatant), anti-D19 (1D3; in-house supernatant), anti-Epcam (G8.8; in-house supernatant), anti-Emr1 (F4/80, in-house supernatant), anti-CD11c (N418; eBioscience), anti-ERTR7 (ERTR7; in-house supernatant) and anti-NeuN (A60; Millipore); and polyclonal antibody to keratin 5 (PRB-160P; Covance), antibody to keratin 14 (PRB-115P-100; Covance), anti-Aire (D-17; Santa Cruz), anti-p63 (poly6190; Biolegend), antibody to STAT1 phosphorylated at Ser727 (S727; Cell Signaling Technology) and Ulex Europaeus Agglutinin (Vector Laboratories). For immunofluorescence, the following detection antibodies were used: Alexa Fluor 594–goat anti-mouse (A-11005; Invitrogen), Alexa Fluor 488–donkey anti-rat (A21208; Molecular Probes), Alexa Fluor 488–donkey anti-rabbit (A21206; Molecular Probes), Alexa Fluor 546–donkey anti-goat (A11056; Molecular Probes), Alexa Fluor 555–donkey anti-rabbit (A31572; Molecular Probes), Alexa Fluor 647–chicken anti-rat (A21472; Molecular Probes), streptavidin–Alexa Fluor 488 (S32354; Molecular Probes) and streptavidin–Alexa Fluor 546 (S11225; Molecular Probes). Images were acquired with an LSM 510 Meta confocal microscope (Ziess).

***In situ* hybridization.** *In situ* hybridization of miR-29 was done as described[45]. Locked nucleic acid probes with 2′O-methyl modifications were used for hybridization to miRNA. Fresh frozen thymus sections 10 µm in thickness were thawed and dried and fixed for 10 min with 4% (vol/vol) paraformaldehyde. After being washed, slides were briefly sunk into acetic anhydrite–TEA solution and washed, followed by prehybridization for 1 h, then hybridization for 30 min. Washes of various stringencies followed, then incubation with 3% (vol/vol) H_2O_2. After slides were washed and blocked, horseradish peroxidase–conjugated antibody to fluorescein isothiocyanate (B13-DE1; Roche) was applied to the slides and signals were amplified after appropriate washing with the TSA system (PerkinElmer). Sections were mounted with Prolong Gold Antifade reagent (Invitrogen).

Luciferase assay. The *Ifnar1* 3′ untranslated region was amplified from genomic DNA, inserted into the PsiCheck2 renilla luciferase reporter plasmid (Promega) and confirmed by sequencing. For reporter assays, HeLa-M cells were cotransfected in triplicate through the use of Lipofectamine 2000 (Invitrogen) with empty PsiCheck2 or PsiCheck2 containing the *Ifnar1* 3′UTR in conjunction with either mouse miR-29a mimic or a mimic control with scrambled sequence (Dharmacon) at a final concentration of 40 nM. Firefly luciferase was used as a normalization control. Reporter activity was detected 24 h after transfection with the Dual-Glo Luciferase Assay System (Promega).

Thymic epithelial expression analysis. Thymic stroma preparations were enriched from three to six pooled thymi[46]. Cells were stained with fluorescein isothiocyanate–conjugated Ulex Europaeus Agglutinin (Vector Labs), phycoerythrin-conjugated anti-BP-1 (6C3; eBioscience), peridinin chlorophyll protein–cyanine 5.5–conjugated anti–I-A–I-E (M5/114; Biolegend), allophycocyanin-conjugated anti-CD45 (104; eBiosciences) and phycoerythrin-indotricarbocyanine-conjugated anti-Epcam (G8.8; Biolegend) and were sorted into cortical epithelium (CD45$^-$MHCII$^+$G8.8$^+$BP-1$^+$UEA$^-$, where 'MHCII' indicates major histocompatibility complex class II) and medullary epithelium (CD45$^-$MHCII$^+$G8.8$^+$BP-1$^-$UEA$^+$). Total RNA was isolated with a miRVana PARIS kit (Ambion), and cDNA was produced with a High Capacity cDNA Reverse Transcription Kit according to the manufacturer's protocol (Applied Biosystems). A Roche LightCycler 480 Sequence Detector based on SYBR green I fluorescence (qPCR MasterMix Plus for SYBR Green I; Eurogentec) was used for quantitative RT-PCR, followed by analysis by the change-in-threshold method ($2^{-\Delta\Delta CT}$)[47]. All mRNA

doi:10.1038/ni.2193

values were normalized to *Actb* mRNA (encoding β-actin); miRNA results were normalized to those of the housekeeping small RNA RNU19.

41. Gordon, J. *et al.* Specific expression of lacZ and cre recombinase in fetal thymic epithelial cells by multiplex gene targeting at the Foxn1 locus. *BMC Dev. Biol.* **7**, 69 (2007).
42. Geboes, L. *et al.* Proinflammatory role of the Th17 cytokine interleukin-22 in collagen-induced arthritis in C57BL/6 mice. *Arthritis Rheum.* **60**, 390–395 (2009).
43. Kelchtermans, H. *et al.* Defective $CD4^+CD25^+$ regulatory T cell functioning in collagen-induced arthritis: an important factor in pathogenesis, counter-regulated by endogenous IFN-gamma. *Arthritis Res. Ther.* **7**, R402–R415 (2005).
44. Dooley, J., Erickson, M. & Farr, A.G. Alterations of the medullary epithelial compartment in the Aire-deficient thymus: implications for programs of thymic epithelial differentiation. *J. Immunol.* **181**, 5225–5232 (2008).
45. Silahtaroglu, A.N. *et al.* Detection of microRNAs in frozen tissue sections by fluorescence in situ hybridization using locked nucleic acid probes and tyramide signal amplification. *Nat. Protoc.* **2**, 2520–2528 (2007).
46. Dooley, J., Erickson, M. & Farr, A.G. An organized medullary epithelial structure in the normal thymus expresses molecules of respiratory epithelium and resembles the epithelial thymic rudiment of nude mice. *J. Immunol.* **175**, 4331–4337 (2005).
47. Livak, K.J. & Schmittgen, T.D. Analysis of relative gene expression data using real-time quantitative PCR and the $2^{-\Delta\Delta CT}$ Method. *Methods* **25**, 402–408 (2001).

doi:10.1038/ni.2193